Tool to recover scalar time-delay systems from experimental time series

M. J. Bünner, M. Popp, Th. Meyer, A. Kittel, and J. Parisi*

Physical Institute, University of Bayreuth, D-95440 Bayreuth, Germany

(Received 8 December 1995; revised manuscript received 31 July 1996)

We propose a method that is able to analyze chaotic time series gained from experimental data. The method allows us to identify scalar time-delay systems. If the dynamics of the system under investigation is governed by a scalar time-delay differential equation of the form $dy(t)/dt = h(y(t), y(t-\tau_0))$, the delay time τ_0 and the function h can be recovered. There are no restrictions to the dimensionality of the chaotic attractor. It turns out that the method is not strongly sensitive to additional noise. We successfully apply the method to various time series taken from a computer experiment and two different electronic oscillators. [S1063-651X(96)50610-0]

PACS number(s): 05.45.+b

Time series analysis of chaotic systems has gained much interest in recent years. Especially, embedding of time series in a reconstructed phase space with the help of time-delayed coordinates was widely used to estimate fractal dimensions of chaotic attractors [1,2] and Lyapunov exponents [3]. It is the advantage of embedding techniques that the time series of only one variable has to be analyzed, even if the investigated system is multidimensional. Furthermore, it can be applied, in principle, to any dynamical system. Unfortunately, the embedding techniques only yield information if the dimensionality of the chaotic attractor under investigation is low. Another drawback is the fact that it does not give any information about the structure of the dynamical system, in the sense that one is able to identify the underlying instabilities. In the following, we propose a method which is taylor-suited to identify scalar systems with a time-delay-induced instability. We will show that the differential equation can be recovered from the time series, if the investigated dynamics obeys a scalar time-delay differential equation. There are no restrictions to the dimensionality of the chaotic attractor. Additionally, the method has the advantage of not being strongly sensitive to noise.

We consider the time evolution of scalar time-delay differential equations

$$\dot{y}(t) = h(y(t), y(t-\tau_0)), \tag{1}$$

with the initial condition

$$y(t) = y_0(t), \quad -\tau_0 < t < 0. \tag{2}$$

The dynamics is supposed to be bounded in the counterdomain $\mathcal{D}$, $y(t) \in \mathcal{D}, \forall \ t$. In Eq. (1), the time derivative of $y(t)$ does not only depend on the state of system at the time t, but there also exist nonlocal correlations in time, because the function h additionally depends on the time-delayed value $y(t-\tau_0)$. These nonlocal correlations in time enable scalar time-delay systems to exhibit a complex time evolution. The number of positive Lyapunov exponents increases

with the delay time τ_0 [4]. Scalar time-delay systems, therefore, constitute a major class of dynamical systems which exhibit hyperchaos [5]. In general, though, the nonlocal correlations in time are not at all obvious from the time series. A state of the system (1) is uniquely defined by a function on an interval of length τ_0. Therefore, the phase space of scalar time-delay systems must be considered as infinite dimensional. The trajectory in the infinite dimensional phase space $\vec{y}(t) = \{y(t'), t-\tau_0 < t' < t\}$ is easily obtained from the time series. The scalar time series $y(t)$, therefore, encompasses the complete information about the trajectory $\vec{y}(t)$ in the infinite dimensional phase space.

The main idea of our analysis method is the following. We project the trajectory $\vec{y}(t)$ from the infinite dimensional phase space to a three-dimensional space which is spanned by the coordinates $[y_{\tau_0} = y(t-\tau_0), y = y(t), \dot{y} = \dot{y}(t)]$. In the $(y_{\tau_0}, y, \dot{y})$ space the differential equation (1) determines a two-dimensional surface h. The projected trajectory $\vec{y}_{\tau_0}(t) = (y(t-\tau_0), y(t), \dot{y}(t))$, therefore, is confined to the surface h and is not able to explore other directions of the $(y_{\tau_0}, y, \dot{y})$ space. From this, we conjecture, that the fractal dimension of the projected attractor has to be between 1 and 2. Furthermore, it follows that any intersection of the chaotic attractor with a surface $k(y_{\tau_0}, y, \dot{y}) = 0$ yields a curve. More precisely spoken, if one transforms the projected trajectory $\vec{y}_{\tau_0}(t)$ to a series of points $\vec{y}_{\tau_0}^i = (y_{\tau_0}^i, y^i, \dot{y}^i)$ that fulfill the condition $k(y_{\tau_0}^i, y^i, \dot{y}^i) = 0$, the series of points $(y_{\tau_0}^i, y^i, \dot{y}^i)$ contracts to a curve and its dimension has to be less than or equal to 1. In general, it cannot be expected that one is able to project a chaotic attractor of arbitrary dimension to a three-dimensional space, in the way that its projection is embedded in a two-dimensional surface. We, nevertheless, demonstrate that this is always possible for chaotic attractors of scalar time-delay systems (1).

In the following, we will show that such a finding can be used to reveal nonlocal correlations in time from the time series. If the dynamics is of the scalar time-delay type (1), the appropriate delay time τ_0 and the function $h(y, y_{\tau_0})$ can be recovered. The trajectory in the infinite dimensional phase space $\vec{y}(t)$ is projected to several three-dimensional

$(y_\tau, y, \dot{y})$ spaces upon variation of τ. The appropriate value $\tau = \tau_0$ is just the one for which the projected trajectory $\vec{y}_\tau$ lies on a surface, representing a fingerprint of the time-delay-induced instability. Projecting the trajectory $\vec{y}$ to the $(y_{\tau_0}, y, \dot{y})$ space, the projected trajectory yields the surface $h(y, y_{\tau_0})$ in the counterdomain $\mathcal{D} \times \mathcal{D}$. With a fit procedure the yet unknown function $h(y, y_{\tau_0})$ can be determined in $\mathcal{D} \times \mathcal{D}$. Therefore, the complete scalar time-delay differential equation has been recovered from the time series. In some cases, it is more convenient to intersect the trajectory $\vec{y}_\tau$ in the $(y_\tau, y, \dot{y})$ space with a surface $k(y_\tau, y, \dot{y}) = 0$, which yields a series of points $\vec{y}_\tau^i = (y_\tau^i, y^i, \dot{y}^i)$. For $\tau = \tau_0$, the points come to lie on a curve and the fractal dimension of the point set has to be less than or equal to 1.

The analysis method is also applicable if noise is added to the time series. The only effect of additional noise is that the projected time series in the $(y_{\tau_0}, y, \dot{y})$ space is not perfectly enclosed in a two-dimensional surface, but the surface is somewhat blurred up. If the analysis is done with an intersected trajectory, the alignment of the noisy data is not perfect. The arguments presented above do not require the dynamics to be settled on its chaotic attractor. Therefore, it is also possible to analyze transient chaotic dynamics. Recently, the coexistence of attractors of time-delay systems has been pointed out [6]. The only requirement for the analysis method is that the trajectory obeys the time-evolution equation (1) which holds for all coexisting attractors in a scalar time-delay system. Therefore, the method is applicable, no matter in which attractor the dynamics has decided to settle. The analysis requires only short time series, which makes it well-suited to be applied on experimental situations. We successfully apply the method to time series gained from a computer experiment and from two different electronic oscillators. We show the robustness of the method to additional noise by analyzing noisy time series.

We numerically calculated the time series of the scalar time-delay differential equation

$$\dot{y}(t) = f(y_{\tau_0}) - g(y), \tag{3}$$

$$f(y_{\tau_0}) = \frac{2.7 y_{\tau_0}}{1 + y_{\tau_0}^{10}} + c_0,$$

$$g(y) = -0.567y + 18.17y^2 - 38.35y^3 + 28.56y^4 - 6.8y^5 - c_0,$$

with the initial condition

$$y(t) = y_0(t), \quad -\tau_0 < t < 0, \tag{4}$$

which is of the form (1) with $h(y_{\tau_0}, y) = f(y_{\tau_0}) - g(y)$. The function g has been chosen to be noninvertible in the counterdomain $\mathcal{D}$. The definition of the functions f and g is ambiguous in the sense that adding a constant c_0 to f can always be cancelled by subtracting c_0 from g without changing h and, therefore, leaving the dynamics of Eq. (3) unchanged. The control parameter is the delay time τ_0. Equation (3) is somewhat similar to the Mackey-Glass equation [7], except for the function g, which is linear in the
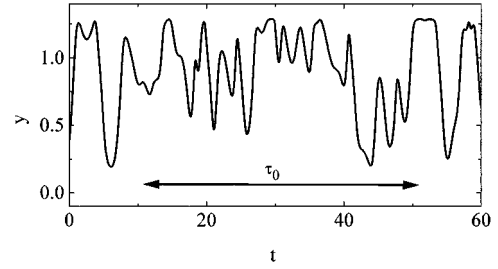

FIG. 1. Time series of the scalar time-delay system (3) obtained from a computer experiment ($\tau_0 = 40.00$).

Mackey-Glass system. Part of the time series is shown in Fig. 1. We used 500 000 data points with a time step of 0.01 for the analysis. The dimension of the chaotic attractor was estimated with the help of the Grassberger-Procaccia algorithm [2] to be clearly larger than 5. To recover the delay time τ_0 and the functions f and g from the time series, we applied the analysis method outlined above. We projected the trajectory $\vec{y}(t)$ from the infinite dimensional phase space to several $(y_\tau, y, \dot{y})$ spaces under variation of τ and intersected the projected trajectory $\vec{y}_\tau$ with the $(y = 1.1)$ plane, which is repeatedly traversed by the trajectory, as can be seen in Fig. 1. The results are the times t^i where the trajectory traverses the $(y = 1.1)$ plane and the intersection points $\vec{y}_\tau^i = (y_\tau^i, 1.1, \dot{y}^i)$. For τ being the appropriate value τ_0, the point set $\vec{y}_{\tau_0}^i$ is correlated via Eq. (3),

$$\dot{y}^i = f(y_{\tau_0}^i) - g(1.1) \tag{5}$$

and, therefore, must have a fractal dimension less than or equal to 1. Then, we ordered the $(y_\tau^i, \dot{y}^i)$ points with respect to the values of y_τ^i. A simple measure for the alignment of the points is the length L of a polygon line connecting all
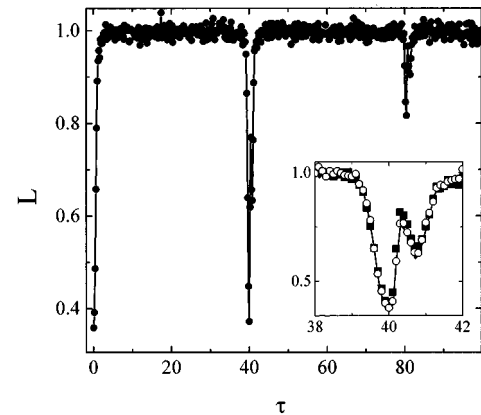

FIG. 2. Length L of the polygon line connecting all ordered points of the projected point set $(y_\tau^i, \dot{y}^i)$ versus τ. L has been normalized so that a maximally uncorrelated point set has the value $L = 1.0$. The inset shows a close-up of the τ axis around the local minimum at $\tau = \tau_0 = 40.00$. Additionally, $L(\tau)$ curves gained from the analysis of noisy time series are shown (no additional noise, straight line; signal-to-noise ratio of 100, open circles; and signal-to-noise ratio of 10, squares).
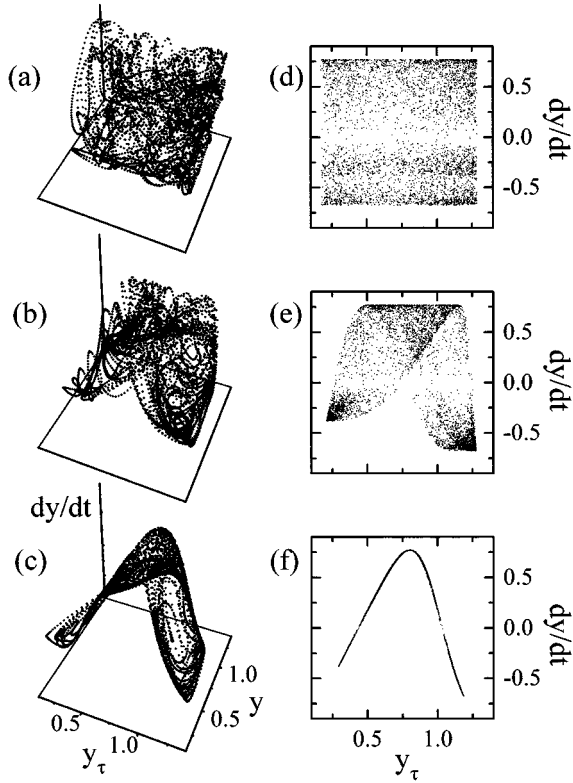
FIG. 3. (a)–(c) Trajectory $\vec{y}_\tau(t)$ which has been projected from the infinite dimensional phase space to the $(y_\tau, y, \dot{y})$ space under variation of τ. (a) $\tau = 20.00$, (b) $\tau = 39.60$, (c) $\tau = \tau_0 = 40.00$. (d)–(f) Projected point set $\vec{y}_\tau^i = (y_\tau^i, \dot{y}^i)$ resulting from the intersection of the projected trajectory $\vec{y}_\tau(t)$ with the $(y = 1.1)$ plane under variation of τ. (d) $\tau = 20.00$, (e) $\tau = 39.60$, (f) $\tau = \tau_0 = 40.00$.

ordered points $(y_\tau^i, \dot{y}^i)$. The length L as a function of τ is shown in Fig. 2. For $\tau = 0$, $L(\tau)$ is minimal, because the points $(y_\tau^i, \dot{y}^i)$ are ordered along the diagonal in the $(y_\tau^i, \dot{y}^i)$ plane. $L(\tau)$ increases with τ and eventually reaches a plateau, where the points $(y_\tau^i, \dot{y}^i)$ are maximally uncorrelated. This is due to short-time correlations of the signal. Eventually, $L(\tau)$ decreases again and shows a dip for τ reaching the appropriate value τ_0. A further decrease of $L(\tau)$ is observed for $\tau = 2\tau_0$. In Figs. 3(a)–3(c), we show the projections $\vec{y}_\tau(t)$ of the trajectory $\vec{y}(t)$ from the infinite dimensional phase space to different $(y_\tau, y, \dot{y})$ spaces under variation of τ. Clearly, for τ approaching the appropriate value τ_0, the appearance of the projected trajectory changes. In Fig. 3(c), the projected trajectory is embedded in a surface which is determined by the function h. In Figs. 3(d)–3(f) we show the point set $(y_\tau^i, \dot{y}^i)$ resulting from the intersection of the projected trajectory $\vec{y}_\tau$ with the $(y = 1.1)$ plane. The point set is projected to the $(y_\tau, \dot{y})$ plane. According to Eq. (5), the points are aligned along the function f for $\tau = \tau_0$. With the appropriate value τ_0, we are in the position to recover the functions f and g from the time series. The functions f and g are ambiguous with respect to the addition of a constant term c_0, as has been outlined above. Therefore, one is free to remove the ambiguity by invoking an additional condition, which we choose to be
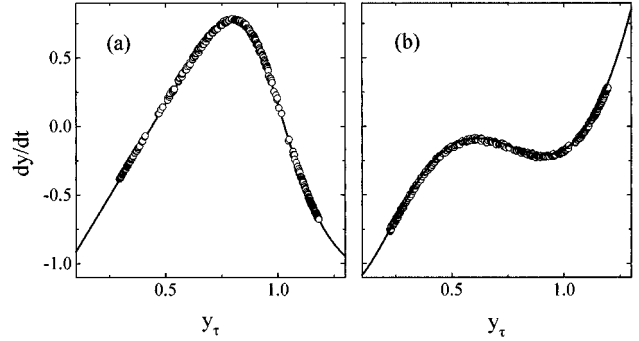

FIG. 4. (a) Comparison of the function f (line) of Eq. (3) with its recovery from the time series (points). (b) Comparison of the function g (solid line) of Eq. (3) with its recovery from the time series (circles).

$$g(1.1) = 0. \tag{6}$$

Then, Eq. (5) reads

$$\dot{y}^i = f(y_{\tau_0}^i). \tag{7}$$

Therefore, function f is recovered by analyzing the intersection points $\vec{y}_{\tau_0}^i$ in the $(\dot{y}, y_{\tau_0})$ plane. To recover the function g, we intersected the time series with the $(y_{\tau_0} = 1.1)$ plane. The resulting point set $\vec{y}_{\tau_0}^j = (\dot{y}^j, y^j)$ is correlated via

$$\dot{y}^j = f(1.1) - g(y^j). \tag{8}$$

The value $f(1.1)$ has been taken from the time series using Eq. (7). In Figs. 4(a)–4(b), we compare the functions f and g as they have been defined in Eq. (3) with the recovery of the functions f and g from the time series. We emphasize that a no fit parameter is involved.

We checked the robustness of the method to additional noise by analyzing noisy time series, which had been produced by adding Gaussian noise to the time series of Eq. (3). We analyzed two noisy time series with a signal-to-noise ratio (SNR) of 10 and 100. In both cases, the additional noise was partially removed with a nearest-neighbor filter (for a SNR of 100, average over six neighbors; for a SNR of 10, average over 20 neighbors). After that, the noisy time series were analyzed in the same way as has been described above. The inset of Fig. 2 shows the result of the analysis. The length L of the polygon line exhibits a local minimum for $\tau = \tau_0$. In the case of the time series with a SNR of 10, the local minimum is again sharp, but somewhat less pronounced. We conjecture that the method is robust with respect to additional noise and, therefore, well suited for the analysis of experimental data.

Finally, we successfully applied the method to experimental time series gained from two different types of electronic oscillators. The first one is the Shinriki oscillator [8,9]. The dynamics of the second oscillator [10] is time-delay induced and mimics the dynamics of the Mackey-Glass equation. In both cases, we intersected the trajectory with the $(\dot{y} = 0)$ plane. The resulting point set was represented in a (y_τ, y) space with different values of τ. Then, we ordered the points
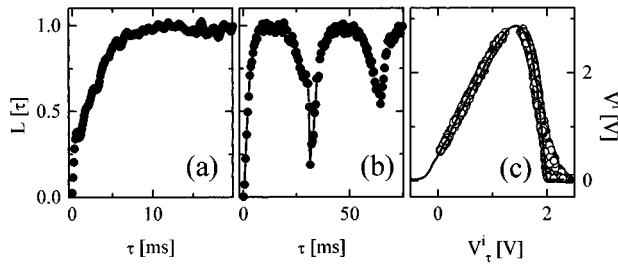
FIG. 5. Length L of the polygon line connecting all ordered points of the projected point set $\vec{y}_\tau^i = (y_\tau^i, y^i)$ versus τ for (a) the Shinriki, and (b) the Mackey-Glass oscillator. $L(\tau)$ has been normalized so that it has the value $L = 1$ for an uncorrelated point set. (c) Comparison of the nonlinear characteristics of the Mackey-Glass oscillator, which is the function $f(y_{\tau_0})$ of an ansatz of the form $h(y, y_{\tau_0}) = f(y_{\tau_0}) + g(y)$, measured directly on the oscillator (line) with its recovery from the time series (dots).

with respect to y_τ and the length L of a polygon line connecting all ordered points (y_τ^i, y^i) was measured. The results are presented in Figs. 5(a) and 5(b). In both cases, $L(\tau)$ has a local minimum for small values of τ as a result of short-range correlations in time. $L(\tau)$ increases in time and reaches a plateau. For the Shinriki oscillator, no further decrease of $L(\tau)$ is observed for increasing τ [Fig. 5(a)]. Such a finding clearly shows that the dynamics of the Shinriki oscillator is not time-delay induced. Analyzing the Mackey-Glass oscillator [Fig. 5(b)], one finds sharp dips in $L(\tau)$ for $\tau = \tau_0$ and $\tau = 2\tau_0$. This is a direct evidence for correlations in time, which are induced by the time delay (for details, see [11]). Obviously, the method is able to identify nonlocal correlations in time from the time series. Eventually, the nonlinear characteristics of the electronic oscillator is compared to its recovery from the time series [Fig. 5(c)].

In conclusion, we have presented a method capable of revealing nonlocal correlations in time of scalar systems by analyzing the time series. If the dynamics of the investigated system is governed by a scalar time-delay differential equation, we are able to recover the scalar time-delay differential equation. There are no constraints on the dimensionality of the attractor. Since scalar time-delay systems are able to exhibit high-dimensional chaos, our method might pave the road to inspecting high-dimensional chaotic systems, where conventional time-series analysis techniques already fail. Furthermore, the motion is not required to be settled on its attractor. The method is not strongly sensitive to additional noise. We have successfully applied the method to time series gained from a computer experiment and to experimental data gained from two different types of electronic oscillators.

While, in general, the verification of dynamical models is a highly complicated task, we have shown that the identification of scalar time-delay systems can be accomplished easily and, thus, allows a detailed comparison of the model equation with experimental time series. In several disciplines, e.g., hydrodynamics [12], chemistry [13], laser physics [14], and physiology [7,15], time-delay effects have been proposed to induce dynamical instabilities. With the help of our method, there is a good chance to verify these models by analyzing the experimental time series. If the dynamics is indeed governed by a time delay, the delay time and the time-evolution equation can be determined. Current and future research activities of the authors concentrate on extending the time-series analysis method to nonscalar time-delay systems as well as to time-delay systems with multiple delay times.

[1] F. Takens, Lect. Notes Math. **898**, 366 (1981).
[2] P. Grassberger and I. Procaccia, Physica D **9**, 189 (1983).
[3] A. Wolf, J. B. Swift, H. L. Swinney, and J. Vastano, Physica D **16**, 285 (1985).
[4] J. D. Farmer, Physica D **4**, 366 (1982).
[5] O. E. Rössler, Z. Naturforsch. **38a**, 788 (1983).
[6] J. Losson, M. C. Mackey, and A. Longtin, CHAOS **3**, 167 (1993).
[7] M. C. Mackey and L. Glass, Science **197**, 287 (1977).
[8] M. Shinriki, M. Yamamoto, and S. Movi, Proc. IEEE **69**, 394 (1981).
[9] B. Reisner, A. Kittel, S. Lück, J. Peinke, and J. Parisi, Z.

Naturforsch. **50a**, 105 (1995).
[10] A. Namajunas, K. Pyragas, and A. Tamasevicius, Phys. Lett. A **201**, 42 (1995).
[11] M. J. Bünner, M. Popp, Th. Meyer, A. Kittel, U. Rau, and J. Parisi, Phys. Lett. A **211**, 345 (1996).
[12] E. Villermaux, Phys. Rev. Lett. **75**, 4618 (1995).
[13] N. Khrustova, G. Veser, and A. Mikhailov, Phys. Rev. Lett. **75**, 3564 (1995).
[14] K. Ikeda and K. Matsumoto, Physica D **29**, 223 (1987).
[15] A. Longtin, J. G. Milton, J. E. Bos, and M. C. Mackey, Phys. Rev. A **41**, 6992 (1990).